



OPEN

Simultaneous activation of CXC chemokine receptor 4 and histamine receptor H1 enhances calcium signaling and cancer cell migration

Chulo Park^{1,2}, Jin-Woo Lee¹, Kiheon Kim¹, Dong-Seung Seen², Jae-Yeon Jeong²✉ & Won-Ki Huh^{1,2,3}✉

C-X-C chemokine receptor 4 (CXCR4) is widely overexpressed in various types of cancer and is involved in several cancer phenotypes including tumor growth, survival, and metastasis. The roles of histamine and histamine receptor H1 (HRH1) in cancer pathogenesis remain controversial. Here, we show that HRH1 is widely expressed in various cancer cell lines and cancer tissues and that coexpression of CXCR4 and HRH1 is associated with poor prognosis in breast cancer. Using bimolecular fluorescence complementation and bioluminescence resonance energy transfer donor saturation assays, we demonstrate that CXCR4 and HRH1 can assemble into a heteromeric complex. Simultaneous activation of CXCR4 and HRH1 synergistically increases calcium flux in MDA-MB-231 cells that endogenously express CXCR4 and HRH1 but not in cells deficient in CXCR4 or HRH1. Costimulation of CXCR4 and HRH1 also significantly enhances CXCL12-induced MDA-MB-231 cell migration, while histamine alone does not induce cell migration. Synergistic effects on calcium flux and cell migration are inhibited by the $G\alpha_i$ inhibitor pertussis toxin and the $G\alpha_q$ inhibitor YM254890, suggesting that the $G\alpha_i$ and $G\alpha_q$ pathways are involved in the synergy. Enhanced calcium signaling and cell migration are also observed in NCI-H23 and HeLa cells, which coexpress CXCR4 and HRH1. Taken together, our findings demonstrate an interplay between CXCR4 and HRH1, and suggest the possibility of the CXCR4-HRH1 heteromer as a potential therapeutic target for anticancer therapy.

G protein-coupled receptors (GPCRs) are the largest family of plasma membrane receptors and mediate most cellular responses to extracellular stimuli, including hormones, neurotransmitters, light, odors, and taste¹. Because GPCRs regulate most physiological responses, they are involved in several pathological pathways. Indeed, over 34% of FDA-approved drugs target GPCRs^{2–4}. GPCRs are also important in cancer, as several GPCRs are known to be responsible for tumor growth, survival, and metastasis⁵.

CXC chemokine receptor 4 (CXCR4) is a chemokine receptor expressed on immune cells that regulates immune cell homing to the bone marrow^{6,7}. CXCR4 is also responsible for breast cancer metastasis to organs that express high levels of its ligand CXCL12, such as lymph nodes, bone marrow, lung, and liver⁸. CXCR4 is widely overexpressed in at least 20 types of cancer, including breast cancer⁹, prostate cancer¹⁰, melanoma¹¹, and neuroblastoma¹². CXCR4 plays important roles in tumor growth¹³, angiogenesis¹⁴, metastasis^{15,16}, and therapeutic resistance¹⁷. Overexpression of CXCR4 is associated with poor prognosis in various cancers such as breast, lung, and colorectal cancers^{18–20}. CXCL12 is also constitutively expressed by cancer-associated fibroblasts in the tumor microenvironment¹⁴, and paracrine signaling between cancer-associated fibroblasts and CXCR4-expressing tumor cells regulates tumor survival and metastasis^{14,21}. Previous studies have shown that CXCR4 function can be regulated through heteromerization with other GPCRs. Cannabinoid receptor type 2 (CB2) inhibits CXCR4-mediated migration through heteromerization with CXCR4 and downregulation of $G\alpha_{13}$ /RhoA

¹School of Biological Sciences, Seoul National University, Seoul 08826, Republic of Korea. ²GPCR Therapeutics Inc., Gwanak-gu, Seoul 08790, Republic of Korea. ³Institute of Microbiology, Seoul National University, Seoul 08826, Republic of Korea. ✉email: jeongjy@gpcr.co.kr; wkh@snu.ac.kr

signaling^{22,23}. CXCR7 forms heteromers with CXCR4 and enhances CXCL12-mediated cell migration through the β -arrestin and ERK pathways²⁴.

Histamine is a biological amine mainly produced by tissue mast cells in response to allergic stimuli²⁵. Histamine triggers allergic reactions, such as vasodilation, increased vascular permeability, bronchoconstriction, and gastric acid secretion, through four types of GPCRs named histamine receptor H1 (HRH1), HRH2, HRH3, and HRH4. HRH1 is ubiquitously expressed and is responsible for classical allergic reactions. HRH2 is highly expressed in immune cells and digestive organs, and is important for immune functions and gastric acid secretion. HRH3 is exclusively expressed in neurons, and HRH4 is mainly expressed in immune cells. Lung, breast, endometrial, colorectal, and melanoma skin cancers exhibit increased levels of histamine and histidine decarboxylase, an enzyme responsible for histamine production^{26–31}. However, histamine treatment produces controversial results in cancer cell proliferation, survival, and migration, depending on the concentrations of histamine and types of histamine receptors^{31–33}.

In the present study, we show that HRH1 is the major histamine receptor highly expressed in many cancer cell lines and cancer tissues and that coexpression of CXCR4 and HRH1 is associated with lower survival in breast cancer by analyzing publicly available RNA-seq databases. We demonstrate that CXCR4 physically interacts with HRH1 using bimolecular fluorescence complementation (BiFC) and bioluminescence resonance energy transfer (BRET) donor saturation assays. Costimulation of CXCR4 and HRH1 synergistically increases calcium flux and CXCL12-induced cell migration in various cancer cells that express CXCR4 and HRH1 endogenously. Using the G α _i inhibitor pertussis toxin and the G α _i inhibitor YM254890, we show that the G α _i and G α _s pathways are involved in the synergistic effects on calcium flux and cell migration. Our results suggest the possibility of the CXCR4-HRH1 heteromer as a potential therapeutic target for anticancer therapy.

Results and discussion

Coexpression of CXCR4 and HRH1 in breast cancer correlates with poor patient prognosis

We first investigated the expression of CXCR4 and HRH1 in cancer. Analysis of publicly available cancer cell line RNA-seq data sourced from the Cancer Cell Line Encyclopedia (CCLE)³⁴ showed that CXCR4 and HRH1 were expressed in 36.2% and 54.2% of 934 cancer cell lines, respectively (Fig. 1A), and that HRH1 was the most frequently and highly expressed histamine receptor of the four HRHs (Fig. 1B). CXCR4 and HRH1 were coexpressed in cell lines from neuroendocrine origin, such as astrocytoma, glioblastoma, medulloblastoma, and neuroblastoma, and in those from other solid cancers, such as bile duct cancer, breast cancer, cecum and colon cancer, gastric cancer, hepatic cancer, mesothelioma, ovarian cancer, pancreatic cancer, renal cancer, thyroid cancer, and uterine cancer (Table S1). CXCR4 and HRH1 were not coexpressed in colorectal cancer, melanoma, multiple myeloma, and prostate cancer cell lines. According to RNA-seq data from The Cancer Genome Atlas (TCGA), CXCR4 was also highly coexpressed with HRH1 in various cancers, such as glioblastoma, renal cancer, mesothelioma, sarcoma, breast cancer, and pancreatic cancer (Fig. 1C). We next investigated the association between coexpression of CXCR4 and HRH1 in cancer and patient prognosis. Kaplan–Meier plots showed that breast cancer patients with high CXCR4 and HRH1 expression had reduced overall survival and progression-free survival compared with other groups (Fig. 1D). These results raise the possibility that coexpression of CXCR4 and HRH1 is associated with breast cancer progression.

CXCR4 physically interacts with HRH1

To understand the potential crosstalk between CXCR4 and HRH1, we examined whether CXCR4 physically interacts with HRH1 using the BiFC assay³⁵. In the BiFC assay, a fluorescent protein is split into two fragments that cannot fluoresce themselves, and each fragment is tagged to the target protein. If two target proteins come into close proximity by physical interaction, then the two tagged fluorescent fragments also become close to each other, and the interaction of the target proteins can be detected by the recovered fluorescence. Consistent with previous reports^{36,37}, coexpression of CXCR4-VN and CXCR4-VC in HEK293A cells resulted in robust BiFC signals at the plasma membrane and cytoplasm, implying the presence of CXCR4 homomers (Fig. 2A, upper panel). Remarkably, BiFC signals were also observed in cells coexpressing CXCR4-VN and HRH1-VC (Fig. 2A, middle panel) or CXCR4-VC and HRH1-VN (Fig. S1A), suggesting that CXCR4 forms heteromers with HRH1. In contrast, BiFC signals were not observed in cells coexpressing CXCR4 and opioid receptor μ type 1 (OPRM1) (Fig. 2A, lower panel), although OPRM1 was expressed well on the cell surface as visualized by antibody staining (Fig. S1B) and flow cytometry (Fig. S1C). These results suggest that CXCR4 physically interacts with HRH1 and that the interaction between CXCR4 and HRH1 is specific.

To further validate the CXCR4-HRH1 interaction, we performed a BRET donor saturation assay^{38,39}. In the BRET donor saturation assay, a fixed concentration of bioluminescent-tagged donor protein and variable concentrations of fluorescent-tagged acceptor protein are expressed in cells. The interaction between two proteins can be examined by quantifying the dependence of the BRET signal on the acceptor/donor expression ratio. Cells expressing increasing concentrations of CXCR4-mCitrine against a fixed amount of CXCR4-Rluc8 exhibited hyperbolic increases in the BRET ratios (Fig. 2B), indicating the formation of CXCR4 homomers. When cells were transfected with increasing amounts of HRH1-mCitrine against a fixed amount of CXCR4-Rluc8, hyperbolic increases in the BRET ratios were obtained (Fig. 2C). Increasing amounts of CXCR4-mCitrine against a fixed amount of HRH1-Rluc8 also led to hyperbolic increases in the BRET ratios (Fig. 2D). In contrast, cells expressing increasing amounts of mCitrine with a fixed amount of CXCR4-Rluc8 or HRH1-Rluc8 showed linear increases in the BRET ratios (Fig. 2B–D), which are indicative of nonspecific random collisions. These results suggest that CXCR4 forms heteromers with HRH1 when they are coexpressed. To our knowledge, this is the first report of CXCR4-HRH1 heteromerization.

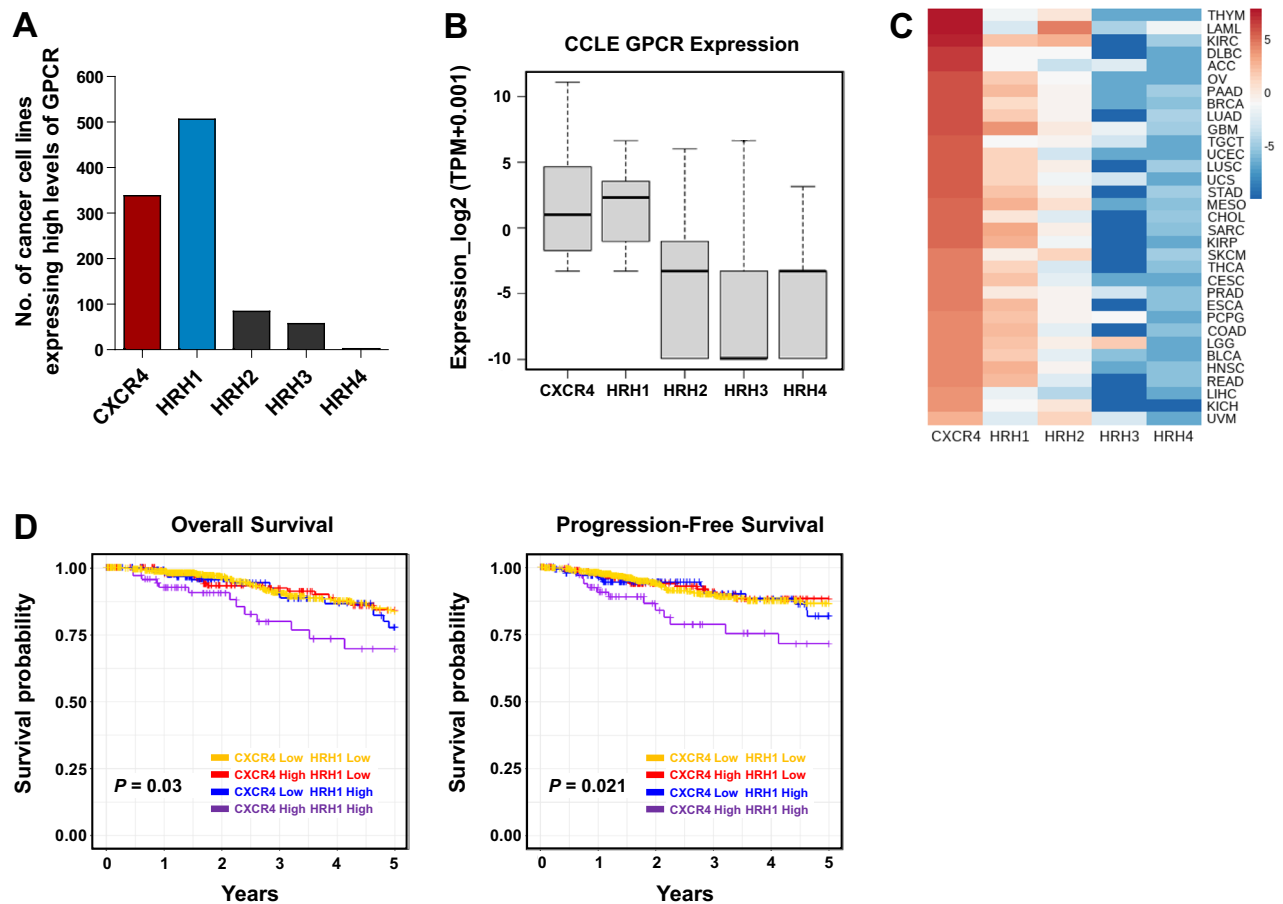


Figure 1. Coexpression of CXCR4 and HRH1 in breast cancers correlates with poor patient prognosis. **(A)** Expression of CXCR4 and histamine receptor subtypes in cancer cell lines based on RNA-seq data from the CCL. Cancer cell lines expressing CXCR4, HRH1, HRH2, HRH3, and HRH4 mRNAs higher than 5 TPM were counted. **(B)** Box plots of the expression levels of CXCR4 and histamine receptors in cancer cell lines from the CCL. **(C)** Heatmap analysis of the expression of CXCR4 and histamine receptors in 33 TCGA cancer types. The median log₂ (TPM + 0.001) values are shown with the scale bar. ACC adrenocortical cancer, BLCA bladder urothelial carcinoma, BRCA breast invasive carcinoma, CESC cervical and endocervical cancer, CHOL cholangiocarcinoma, COAD colon adenocarcinoma, DLBC diffuse large B-cell lymphoma, ESCA esophageal carcinoma, GBM glioblastoma multiforme, HNSC head and neck squamous cell carcinoma, KICH kidney chromophobe, KIRC kidney clear cell carcinoma, KIRP kidney papillary cell carcinoma, LAML acute myeloid leukemia, LGG brain lower grade glioma, LIHC liver hepatocellular carcinoma, LUAD lung adenocarcinoma, LUSC lung squamous cell carcinoma, MESO mesothelioma, OV ovarian serous cystadenocarcinoma, PAAD pancreatic adenocarcinoma, PCPG pheochromocytoma and paraganglioma, PRAD prostate adenocarcinoma, READ rectum adenocarcinoma, SARC sarcoma, SKCM skin cutaneous melanoma, STAD stomach adenocarcinoma, TGCT testicular germ cell tumor, THCA thyroid carcinoma, THYM thymoma, UCEC uterine corpus endometrioid carcinoma, UCS uterine carcinosarcoma, UVM uveal melanoma. **(D)** Coexpression of CXCR4 and HRH1 reduces overall survival and progression-free survival in breast cancer. Kaplan–Meier survival curves were analyzed using clinical data from TCGA Breast Invasive Carcinoma. Patients were divided into four groups according to the expression of CXCR4 and HRH1, and comparisons between groups were performed by the log-rank test. Pooled log-rank *P* values are presented for overall survival (left panel) and progression-free survival (right panel).

CXCR4 and HRH1 are endogenously coexpressed in the breast cancer cell line MDA-MB-231

To investigate the role of the CXCR4–HRH1 heteromer in cancer cells, we examined the endogenous expression of CXCR4 and histamine receptors in MDA-MB-231 breast cancer cells using real-time quantitative PCR (RT–qPCR). Significant levels of CXCR4 and HRH1 mRNAs were detected in MDA-MB-231 cells, while mRNAs for other histamine receptors were undetectable (Fig. 3A). In addition, histamine-induced calcium flux was completely reduced by the HRH1-selective antagonist pyrilamine but not by the HRH2-selective antagonist ranitidine, the HRH3-selective antagonist pitolisant, or the HRH4-selective antagonist JNJ-777120 (Fig. S2). These results suggest that HRH1 is the main histamine receptor responsible for histamine-induced calcium flux in MDA-MB-231 cells.

Next, we investigated whether CXCR4 and HRH1 proteins are expressed in MDA-MB-231 cells. CXCR4 expression on the surface of MDA-MB-231 cells was successfully detected by flow cytometry using an

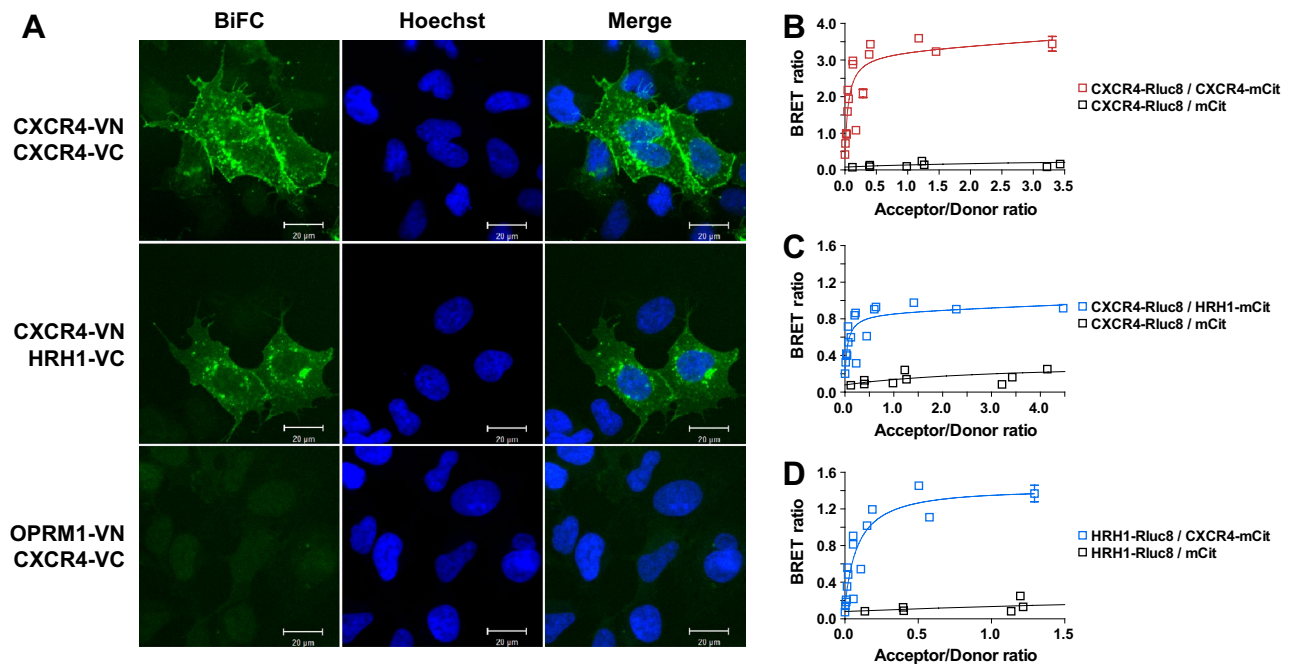


Figure 2. HRH1 physically interacts with CXCR4. (A) Analysis of CXCR4-HRH1 heteromerization using the BiFC assay. HEK293A cells were transfected with CXCR4-VN and CXCR4-VC (upper panel), CXCR4-VN and HRH1-VC (middle panel), or OPRM1-VN and CXCR4-VC (lower panel), and BiFC signals were visualized. Cell nuclei were stained with Hoechst 33342. Images are representative of three independent experiments. (B–D) Analysis of CXCR4-HRH1 heteromerization using the BRET donor saturation assay. BRET donor saturation curves of CXCR4 homomer (B) and CXCR4-HRH1 heteromer (C,D) were obtained with HEK293A cells transfected with a fixed amount of donor (GPCR-Rluc8) and increasing amounts of acceptor (GPCR-mCitrine) plasmids. BRET values were plotted as a function of mCitrine/Rluc8. The curves were fitted using a nonlinear regression equation assuming a single binding site and represent three independent experiments.

anti-CXCR4 antibody (Fig. 3B, upper panel). When the CXCR4 gene was deleted by CRISPR/Cas9, the surface expression of CXCR4 was completely lost (Fig. 3B, lower panel). Flow cytometry using an anti-HRH1 antibody also demonstrated that HRH1 was expressed in MDA-MB-231 cells (Fig. 3C, upper panel) and that its expression was lost upon deletion of HRH1 by CRISPR/Cas9 (Fig. 3C, lower panel). Consistent with these observations, CXCL12 failed to induce calcium flux in CXCR4-deficient MDA-MB-231 cells (Fig. 3D) and histamine-induced calcium flux was also lost in HRH1-deficient MDA-MB-231 cells (Fig. 3E). These results indicate that CXCR4 and HRH1 are endogenously expressed in MDA-MB-231 cells and mediate proper calcium mobilization.

Costimulation of CXCR4 and HRH1 induces synergistic calcium flux in MDA-MB-231 cells

It has been reported that CXCR4-mediated calcium signaling regulates cell migration and survival^{40–42}. HRH1 also induces calcium signaling via G_{α_q} protein and phospholipase C (PLC)^{43,44}. To investigate whether calcium signaling induced by CXCR4 is affected by HRH1 or vice versa, MDA-MB-231 cells were stimulated with CXCL12 and histamine, and intracellular calcium flux was measured. Interestingly, calcium flux induced by simultaneous treatment with CXCL12 and histamine was significantly higher than the sum of calcium flux induced by CXCL12 and histamine alone (Fig. 4A). The addition of histamine markedly increased CXCL12-induced calcium flux at all CXCL12 doses in control cells, while this increase was not observed in cells deficient in HRH1 (Fig. 4B) or CXCR4 (Fig. S3A). Similarly, the addition of CXCL12 slightly increased histamine-induced calcium flux in control cells but not in cells deficient in CXCR4 (Fig. 4C) or HRH1 (Fig. S3B). Consistent with these observations, the CXCR4 antagonist AMD3100 and the HRH1 antagonist pyrilamine abolished calcium flux in MDA-MB-231 cells in a dose-dependent manner (Fig. 4D). Taken together, these results suggest that both CXCR4 and HRH1 are important for the synergistic calcium flux induced by CXCL12 and histamine cotreatment. We also examined whether HRH1 affects CXCR4-mediated $G_{\alpha_{i/o}}$ signaling, which is another major downstream signaling pathway of CXCR4. As expected, forskolin-induced cAMP production was reduced by CXCL12 (Fig. S4). However, the addition of histamine did not affect CXCR4-mediated cAMP responses. This result suggests that HRH1 affects CXCR4-mediated calcium signaling but not cAMP signaling.

Both the $G_{\alpha_{i/o}}$ and $G_{\alpha_{q/11}}$ pathways are important for synergistic calcium flux induced by costimulation of CXCR4 and HRH1

To understand the signaling pathways that regulate synergistic calcium flux upon costimulation of CXCR4 and HRH1, MDA-MB-231 cells were treated with inhibitors that block Ga activation. Pretreatment with vehicle alone had no effect on CXCL12-histamine-induced synergistic calcium mobilization (Fig. 5A). Consistent with previous reports that the $G_{\alpha_{i/o}}$ inhibitor pertussis toxin (PTX) inhibits CXCL12/CXCR4-mediated calcium

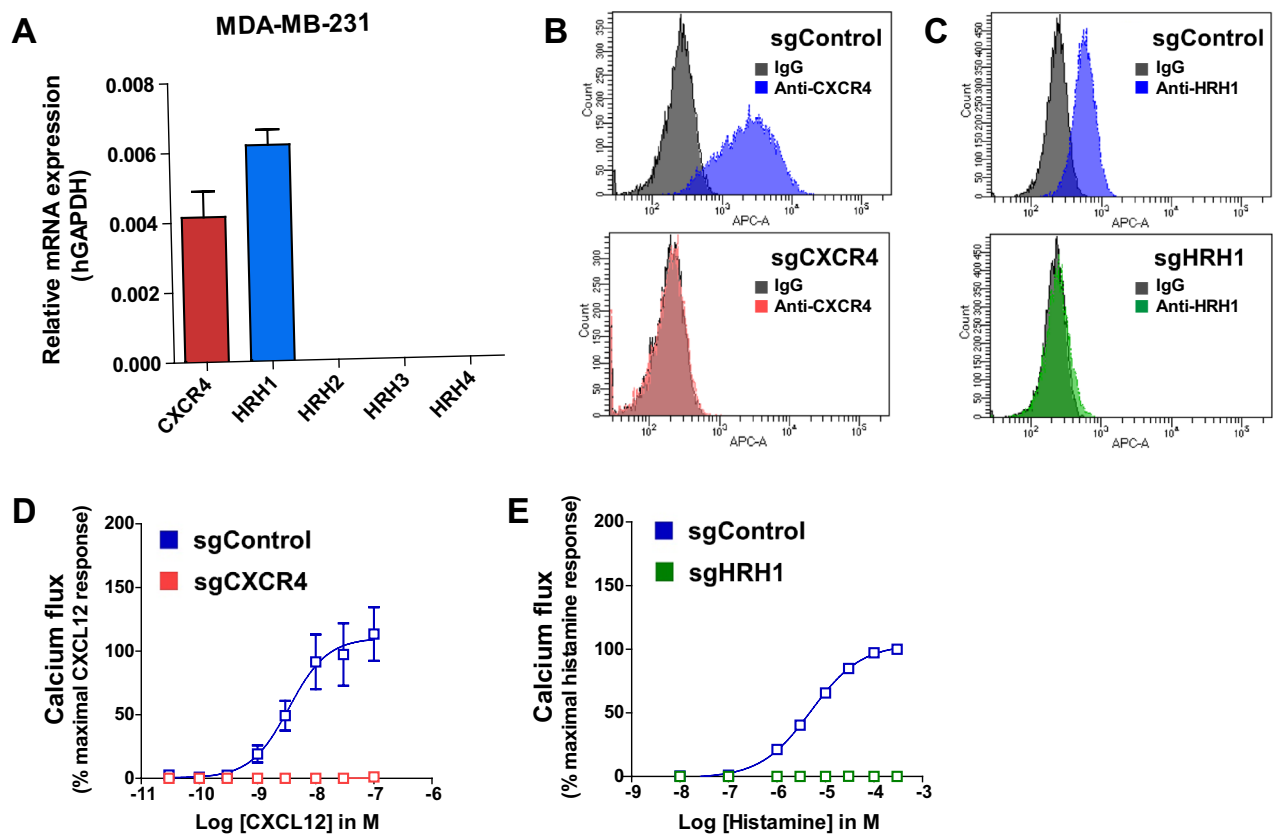


Figure 3. CXCR4 and HRH1 are endogenously coexpressed in MDA-MB-231 breast cancer cells. (A) Analysis of the mRNA expression of CXCR4 and histamine receptors in MDA-MB-231 cells using RT–qPCR. Endogenous β -actin was used to normalize the expression of target genes. (B,C) Expression of CXCR4 and HRH1 proteins in MDA-MB-231 cells. Cells were transduced with lentiviruses encoding CRISPR/Cas9 and nontargeting single guide RNA (sgControl), CXCR4-targeting single guide RNA (sgCXCR4), or HRH1-targeting single guide RNA (sgHRH1). After puromycin selection, cells were stained with an anti-CXCR4 antibody (B) or an anti-HRH1 antibody (C). (D,E) Functional expression of CXCR4 and HRH1 in MDA-MB-231 cells. Cells were stimulated with increasing doses of CXCL12 (D) or histamine (E), and calcium flux was measured. Data are expressed as mean \pm s.e.m. ($n = 3$).

signaling^{45,46}, pretreatment with PTX completely blocked CXCL12-induced calcium flux, while it did not affect histamine-induced calcium flux (Fig. 5B). Notably, PTX pretreatment abolished the synergistic increase in calcium flux induced by CXCL12 and histamine cotreatment, suggesting that $G_{\alpha_{i/o}}$ activation is essential not only for CXCL12-induced calcium mobilization but also for CXCL12-histamine-induced synergistic calcium flux. When cells were pretreated with the $G_{\alpha_{q/11}}$ inhibitor YM254890, both CXCL12- and histamine-induced calcium fluxes were inhibited (Fig. 5C), suggesting that $G_{\alpha_{q/11}}$ activation is crucial for CXCR4- and HRH1-mediated calcium signaling. CXCL12-histamine-induced synergistic calcium mobilization was also considerably reduced by YM254890 pretreatment. Given the above results showing that synergistic calcium flux induced by CXCL12 and histamine cotreatment was abolished by PTX and YM254890 (Fig. 5B–D), it is likely that activation of both $G_{\alpha_{i/o}}$ and $G_{\alpha_{q/11}}$ is important for increased calcium signaling upon costimulation of CXCR4 and HRH1. Consistent with our results, Pfeil et al.⁴⁷ have recently reported that activation of both the G_{α_i} and G_{α_q} pathways results in synergistic calcium signaling; when G_{α_i} - and G_{α_q} -coupled GPCRs are coactivated, the occluded catalytic site of PLC β is freed by G_{α_q} , leading to amplification of calcium signaling mediated by $G\beta\gamma$ -PLC β . Whether the physical interaction between CXCR4 and HRH1 affects synergistic calcium flux due to the signaling crosstalk between the G_{α_i} and G_{α_q} pathways is not yet clear and will need further investigation.

Costimulation of CXCR4 and HRH1 enhances CXCR4-mediated migration of MDA-MB-231 cells

CXCL12/CXCR4-mediated cell migration plays an important role in cancer metastasis to distant organs and in drug resistance by mobilizing cancer cells to niches rich in survival-promoting factors^{14,20,48–50}. Therefore, we investigated whether costimulation of CXCR4 and HRH1 affects CXCL12/CXCR4-mediated cell migration of MDA-MB-231 cells using a transwell migration assay. As expected, CXCL12 (3 nM) induced MB-231 cell migration, while histamine (100 nM) did not (Fig. 6A,B). Notably, however, histamine significantly enhanced CXCL12-induced migration. CXCL12 induced MDA-MB-231 cell migration in a dose-dependent manner with maximal migration at 10 nM (Fig. 6C). The addition of 100 nM histamine significantly increased CXCL12-induced migration at all CXCL12 doses tested. When cells were pretreated with the HRH1 antagonist pyrilamine,

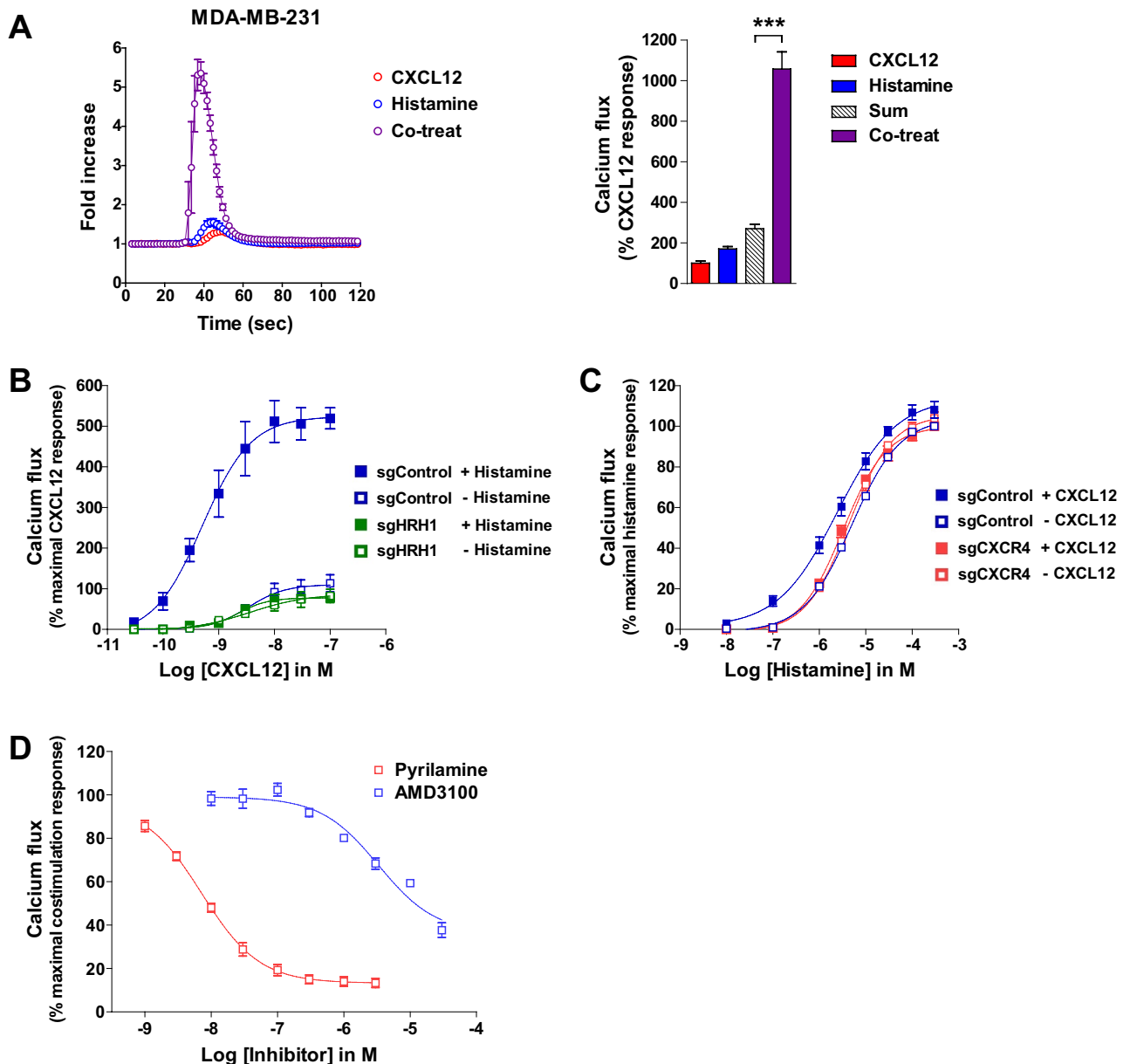


Figure 4. Costimulation of CXCR4 and HRH1 induces synergistic calcium mobilization in MDA-MB-231 cells. **(A)** MDA-MB-231 cells were stimulated with 3 nM CXCL12, 100 nM histamine, or both agonists at the same concentrations, and intracellular calcium flux was measured (left panel). The area under the curve of each calcium response was calculated and normalized to that of CXCL12 (right panel). Data are expressed as mean \pm s.e.m. ($n = 3$). $***P < 0.001$. **(B,C)** Synergistic calcium flux is mediated by CXCR4 and HRH1. Intracellular calcium flux was measured by stimulating HRH1 knockout (sgHRH1) or control (sgControl) cells with increasing concentrations of CXCL12 in the absence or presence of 100 nM histamine **(B)**. Intracellular calcium flux was measured by stimulating CXCR4 knockout (sgCXCR4) or control (sgControl) cells with increasing concentrations of histamine in the absence or presence of 3 nM CXCL12 **(C)**. Data are expressed as mean \pm s.e.m. ($n = 3-6$). **(D)** Inhibition of the calcium response by the CXCR4 antagonist AMD3100 and the HRH1 antagonist pyrilamine. MDA-MB-231 cells were pretreated with increasing concentrations of AMD3100 or pyrilamine, and costimulated with 3 nM CXCL12 and 100 nM histamine. Data are expressed as mean \pm s.e.m. ($n = 3$).

the effect of histamine on CXCL12-induced migration was abolished (Fig. 6D), demonstrating that the effect of histamine is mediated by HRH1.

Next, to understand the signaling pathways involved in enhanced cell migration by cotreatment with CXCL12 and histamine, we investigated the effects of the $G_{\alpha_{i/o}}$ inhibitor PTX and the $G_{\alpha_{q/11}}$ inhibitor YM254890 on MDA-MB-231 cell migration. Consistent with previous reports that $G_{\alpha_{i/o}}$ signaling is important for CXCL12-induced migration^{51,52}, PTX completely inhibited not only CXCL12-induced migration but also histamine-enhanced CXCL12-induced migration (Fig. 7A,B). In contrast, YM254890 selectively abrogated histamine-enhanced

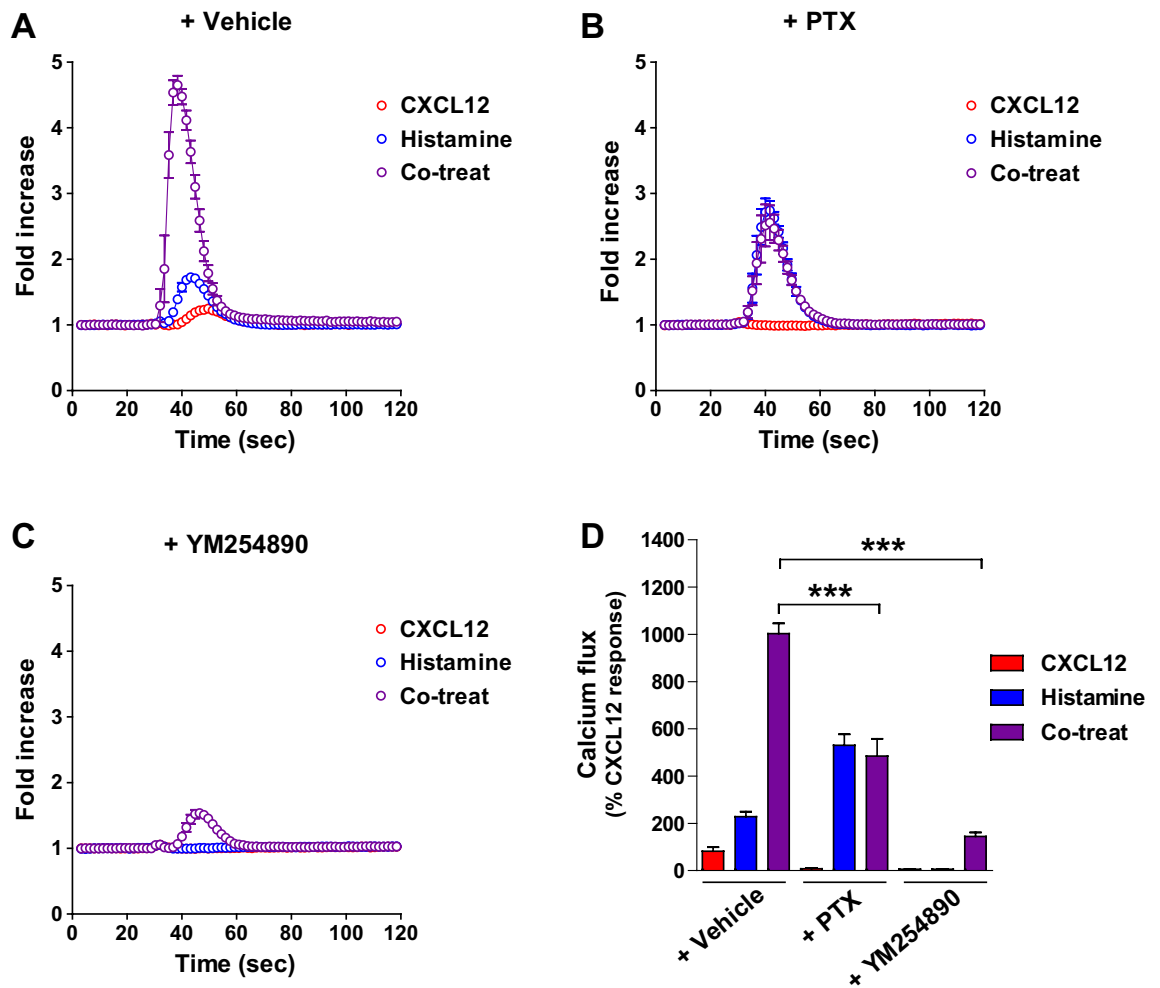


Figure 5. Activation of both $G_{\alpha_{i/o}}$ and $G_{\alpha_{q/11}}$ is important for synergistic calcium mobilization induced by costimulation of CXCR4 and HRH1. MDA-MB-231 cells were pretreated with vehicle (A), PTX (100 ng/ml, overnight) (B), or YM254890 (300 nM, 30 min) (C) prior to agonist treatment. Cells were stimulated with 3 nM CXCL12, 100 nM histamine, or both, and intracellular calcium flux was measured. (D) The area under the curve of each calcium response was calculated and normalized to that of CXCL12. Data are expressed as mean \pm s.e.m. ($n = 3$). *** $P < 0.001$.

CXCL12-induced migration (Fig. 7C), suggesting that $G_{\alpha_{q/11}}$ activation is required for histamine-enhanced CXCL12-induced migration. These results suggest that the $G_{\alpha_{i/o}}$ and $G_{\alpha_{q/11}}$ pathways, which are shown above to be important for calcium signaling, also play major roles in enhanced CXCR4-mediated cell migration upon costimulation of CXCR4 and HRH1.

The synergistic effect of CXCR4 and HRH1 on calcium signaling and cell migration is observed in other cancer cell lines

To investigate whether enhanced calcium signaling and cell migration by concurrent treatment with CXCL12 and histamine are conserved in other cancer cell lines, we measured the expression of CXCR4 and HRH1 using RT-qPCR in NCI-H23 lung cancer cells, A-498 renal cancer cells, SNU-423 hepatocellular carcinoma cells, HeLa cervical cancer cells, COLO 205 colon cancer cells, and Calu-3 lung cancer cells. CXCR4 was highly expressed in all cell lines examined (Fig. 8A, upper panel). The expression of HRH1 was also high in NCI-H23, A-498, SNU-423, and HeLa cells, but was relatively low in COLO 205, and Calu-3 cells (Fig. 8A, lower panel).

Next, we examined calcium signaling and cell migration in these cancer cell lines. CXCL12 induced calcium flux in most cancer cell lines except SNU-423 cells (Fig. 8B), although SNU-423 cells showed similar levels of CXCR4 expression to NCI-H23, COLO 205, and Calu-3 cells. Histamine induced calcium flux in all cells. Notably, synergistic calcium flux was observed in NCI-H23, and HeLa cells. Intriguingly, while A-498 cells responded to CXCL12 with robust calcium flux, they did not show synergistic calcium flux upon simultaneous treatment with CXCL12 and histamine. It seems likely that calcium flux and its modulation are influenced by the cellular context, including membrane lipid composition and differential expression of receptor-interacting proteins, such as G protein subtypes, GPCR kinases, and PLC β isoforms. NCI-H23 and HeLa cells also exhibited significantly enhanced cell migration upon simultaneous treatment with CXCL12 and histamine (Fig. 8C–F). Taken together,

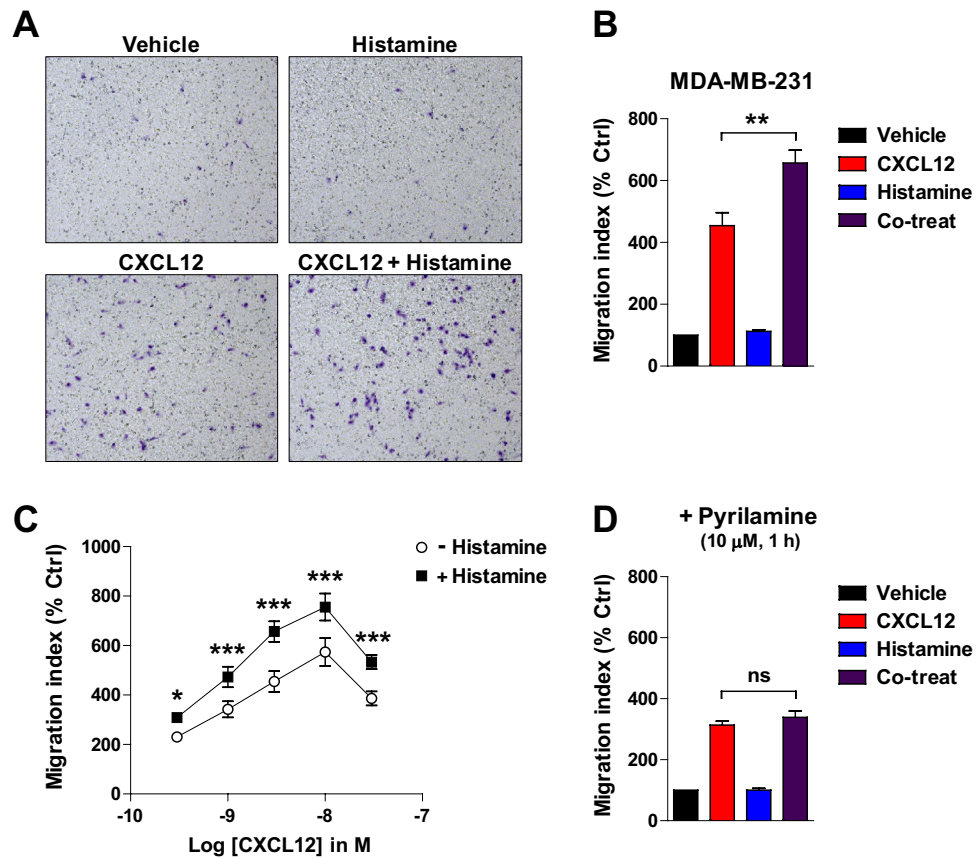


Figure 6. Costimulation of CXCR4 and HRH1 enhances CXCR4-mediated migration of MDA-MB-231 cells. (A) Representative images of MDA-MB-231 cells migrated by vehicle, 3 nM CXCL12, 100 nM histamine, or both agonists. (B) Quantification of migration shown in (A). Data are expressed as mean \pm s.e.m. ($n=3$). $**P<0.01$. (C) CXCL12-induced cell migration in the absence or presence of 100 nM histamine. $*P<0.05$; $***P<0.001$. (D) Cells were treated with 10 μ M pyrilamine for 1 h before the migration assay with 3 nM CXCL12, 100 nM histamine, or both. Data are expressed as mean \pm s.e.m. ($n=3$). *Ns* not significant.

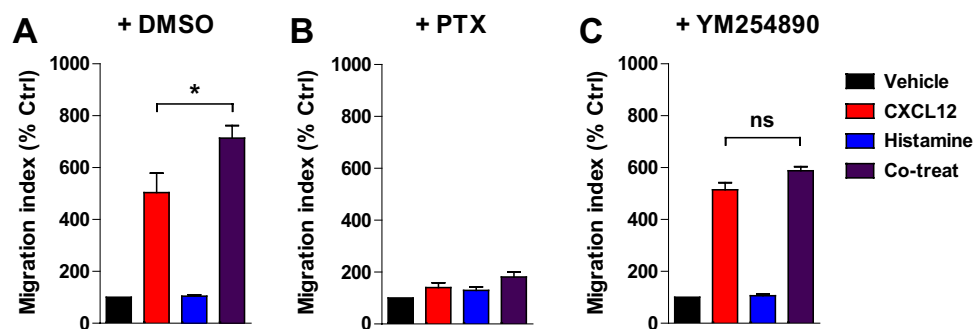


Figure 7. $G\alpha_{i/o}$ plays a fundamental role in CXCR4-mediated migration and $G\alpha_{q/11}$ is responsible for enhanced cell migration induced by costimulation of CXCR4 and HRH1. Cells were treated with vehicle (A), PTX (100 ng/ml, overnight) (B), or YM254890 (300 nM, 30 min) (C) before the migration assay with 3 nM CXCL12, 100 nM histamine, or both. Data are expressed as mean \pm s.e.m. ($n=3$). $*P<0.05$; *ns*, not significant.

these results suggest that the synergistic effect of CXCR4 and HRH1 costimulation on calcium signaling and cell migration could be shared by several cancer cell lines.

In conclusion, our findings provide new insights into the role of HRH1 in the CXCL12/CXCR4 signaling pathway. CXCL12 is constitutively expressed by cancer-associated fibroblasts in the tumor microenvironment¹⁴, binds to CXCR4-expressing tumor cells, and mediates several cancer phenotypes, including proliferation, epithelial to mesenchymal transition, neangiogenesis, and tumor cell migration²¹. In contrast, the roles of histamine and

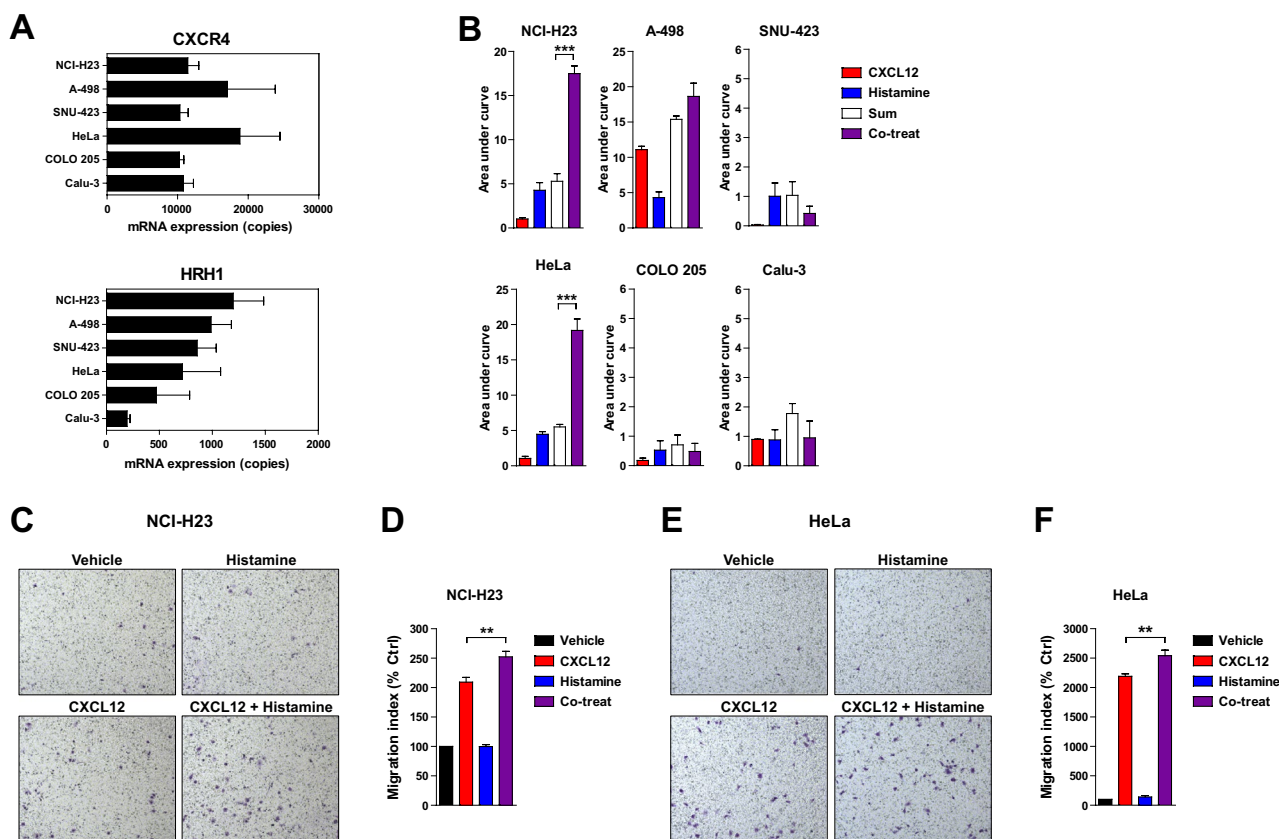


Figure 8. The synergistic effect of CXCR4 and HRH1 on calcium signaling and cell migration has been observed in other cancer cell lines. (A) RT–qPCR analysis of the expression of CXCR4 (upper panel) and HRH1 (lower panel) in NCI-H23, A-498, SNU-423, HeLa, COLO 205, and Calu-3 cells. Data are expressed as mean \pm s.e.m. ($n = 3$). (B) Cells were stimulated with 3 nM CXCL12, 100 nM histamine, or both, and intracellular calcium flux was measured. The area under the curve of each calcium response was calculated and normalized to that of CXCL12. Data are expressed as mean \pm s.e.m. ($n = 3$). $***P < 0.001$. (C) Representative images of NCI-H23 cells migrated by vehicle, 10 nM CXCL12, 100 nM histamine, or both agonists. (D) Quantification of migration shown in (C). Data are expressed as mean \pm s.e.m. ($n = 3$). $**P < 0.01$. (E) Representative images of HeLa cells migrated by vehicle, 10 nM CXCL12, 100 nM histamine, or both agonists. (F) Quantification of migration shown in (E). Data are expressed as mean \pm s.e.m. ($n = 3$). $**P < 0.01$.

HRH1 in cancer pathology are controversial. Histamine either inhibits or stimulates cancerous phenotypes in a dose-dependent manner^{53,54}. HRH1 also has both anticancer^{32,55,56} and procancer effects^{33,57,58}. These controversies suggest that HRH1 does not function alone but may crosstalk with other signaling pathways. In the present study, we demonstrate that HRH1 physically interacts with CXCR4 and that the histamine/HRH1 pathway is functionally related to the CXCL12/CXCR4 pathway. Given that histamine is ubiquitously present in various tissues⁵⁹, it is highly probable that CXCR4 and HRH1 in tumor cells that express both GPCRs can be simultaneously stimulated. Once coactivated, CXCR4 and HRH1 may contribute to tumor progression by enhancing calcium signaling and cell migration. Therefore, our findings suggest that the CXCR4–HRH1 heteromer may serve as a potential therapeutic target for anticancer therapy. Because antihistamines are commonly prescribed drugs and their safety has been proven for a long time, it will be worth investigating whether antihistamines can be repositioned for cancer treatment.

Materials and methods

Cell culture and reagents

MDA-MB-231 cells were purchased from the American Type Culture Collection (Rockville, MD). NCI-H23, A-498, SNU-423, HeLa, COLO 205, and Calu-3 cells were purchased from the Korean Cell Line Bank (Seoul, Korea). HEK293A cells were purchased from Invitrogen (Carlsbad, CA). MDA-MB-231, NCI-H23, A-498, SNU-423, and COLO 205 cells were cultured in RPMI 1640 supplemented with 10% fetal bovine serum (FBS), 100 U/mL penicillin, and 100 μ g/mL streptomycin at 37 $^{\circ}$ C in 5% CO₂. HeLa cells were grown in modified Eagle's medium (MEM; HyClone, Logan, UT) supplemented with 10% FBS, penicillin, and streptomycin. HEK293A and Calu-3 cells were cultured in Dulbecco's modified Eagle's medium (DMEM; HyClone) supplemented with 10% FBS, penicillin, and streptomycin. CXCL12 (#300-28A) was purchased from PeproTech (London, UK). Histamine (#H7250) was purchased from Sigma–Aldrich (St. Louis, MO). AMD3100 (#HY10046), U73122 (#HY-13419), and U0126 (#HY-12031) were purchased from MedChemExpress (Monmouth Junction, NJ). Pyrilamine (#0660)

and PTX (#3097) were purchased from Tocris Bioscience (Ellisville, MO). YM254890 (#AG-CN2-0509-MC05) was purchased from AdipoGen Life Sciences (San Diego, CA).

BiFC assay

The bimolecular fluorescence complementation (BiFC) assay is a technique to detect protein–protein interactions in living cells in which two complementary N- and C-terminal fragments of fluorescent protein reconstitute a fluorescent signal only when both fragments are close together through interaction between the two different proteins to which they are fused³⁵. Vectors containing the BiFC fragments (pCS2 + VNm10 and pBiFC-VC155) were obtained from James Smith⁶⁰ and Chang-Deng Hu³⁵. The complementary fragments of Venus protein (VNm10, VC155) were subcloned at the C-termini of CXCR4, HRH1, and OPRM1. For the BiFC experiments, HEK293A cells (1×10^4 cells/well) were seeded onto a 96-well black clear-bottom microplate (#3340) purchased from Corning (Corning, NY). The next day, cells were cotransfected with complementation pairs (CXCR4-VN/CXCR4-VC, CXCR4-VN/HRH1-VC, HRH1-VN/CXCR4-VC, CXCR4-VN/HA-OPRM1-VC, or HA-OPRM1-VN/CXCR4-VC). 48 h after transfection, the cells were fixed with 2% formaldehyde and stained with Hoechst 33342 (Invitrogen). Rabbit anti-HA monoclonal antibody (#3724, Cell Signaling Technology, Beverly, MA) was used to detect the cell surface expression of N-terminal HA-tagged OPRM1-VN and -VC constructs. Briefly, fixed cells were blocked in DPBS containing 1% BSA and immunostained overnight at 4 °C. Cells were washed twice and labeled with goat anti-rabbit IgG-Alexa Fluor 568 antibody (#A11011, Invitrogen) for 1 h at room temperature. Cells were washed twice after secondary antibody incubation, and BiFC, cell surface immunofluorescence, and nuclear images were captured using a Zeiss LSM 700–2 confocal microscope (40 \times objective).

BRET donor saturation assay

In the BRET donor saturation assay, a fixed concentration of bioluminescent-tagged donor protein and variable concentrations of fluorescent-tagged acceptor protein are expressed in cells. The interaction between two proteins can be examined by quantifying the dependence of the BRET signal on the acceptor/donor expression ratio^{38,39}. HEK293A cells were seeded onto 24-well plates. The next day, cells were transfected with the BRET donor (3, 10, 30, 100 ng of GPCR-Rluc8) and the BRET acceptor (0, 10, 30, 100, 300 ng of GPCR-mCitrine). Transfections were performed using Lipofectamine 2000 (Invitrogen). The total amount of transfected DNA was fixed to 400 ng using empty vector. 24 h after transfection, the cells were detached in assay buffer (DMEM without phenol red, 20 mM HEPES) and distributed onto 96-well white microplates (#3917; 4×10^4 cells/well) purchased from Corning. The next day, acceptor expression in each cell was measured with excitation 485/14, emission 535/25 using Tristar2 microplate reader (Berthold Technologies, Bad Wildbad, Germany). Next, the Rluc8 substrate coelenterazine h (NanoLight Technology, Pinetop, AZ) was added at a final concentration of 5 μ M. Cells were further incubated for an additional 5 min before BRET measurements. BRET measurements were also performed using a TriStar2 microplate reader. The acceptor/donor ratios of each transfected cell were calculated by dividing mCitrine relative fluorescence unit (RFU) by Rluc8 relative luminescence unit (RLU).

Gene knockout using the CRISPR/Cas9 system

Nontargeting single guide RNA (sgControl; 5'-ACGGAGGCTAAGCGTCGCAA-3'), CXCR4-targeting single guide RNA (sgCXCR4; 5'-ACTTACTGATCCCCCTCCA-3'), or HRH1-targeting single guide RNA (sgHRH1; 5'-CGATCAAGTCCGCCACCGAG-3') cloned in pLentiCRISPRv2 vectors were purchased from Genscript (Piscataway, NJ). The pLentiCRISPRv2 plasmid for each single guide RNA was cotransfected into HEK293T cells with packaging plasmids for lentiviral production. MDA-MB-231 cells transduced with lentiviruses containing sgControl, sgCXCR4, or sgHRH1 were cultured for 2 weeks with puromycin selection (1 μ g/ml). Knockout of CXCR4 or HRH1 genes was validated using flow cytometry and calcium flux assays.

Calcium flux assay

Intracellular calcium mobilization was measured using Cal-520 AM calcium staining dye (AAT Bioquest, Sunnyvale, CA) according to the manufacturer's directions. Briefly, MDA-MB-231 cells (4×10^4 cells/well) were seeded into a 96-well black clear-bottom microplate (#3340, Corning). After 48 h, the cells were stained with Cal-520 AM dye diluted in assay buffer (HBSS, 0.1% BSA, 20 mM HEPES) for 2 h at 37 °C. After staining, the cells were washed with assay buffer, and inhibitors or vehicle were pretreated for 30 min. In the case of PTX pretreatment, the cells were pretreated overnight the day before staining. Intracellular calcium flux was measured by a Flexstation 3 microplate reader (Molecular Devices, San Jose, CA).

cAMP signaling assay

Intracellular cAMP signaling was measured using the GloSensor-22F cAMP reporter (Promega, Madison, WI). MDA-MB-231 cells transduced with lentiviruses containing the GloSensor-22F were cultured for 2 weeks with hygromycin selection (200 μ g/ml). The day before experiments, MDA-MB-231 cells expressing the biosensor were seeded into a 96-well white microplate (#3917, Corning) and incubated at 37 °C and 5% CO₂. The next day, the culture medium was replaced with assay buffer containing 0.1% BSA and 2% GloSensor cAMP reagent in CO₂-independent medium (Gibco, Gaithersburg, MD). After 2 h of incubation at room temperature, intracellular cAMP was measured using a TriStar2 microplate reader.

RT–qPCR

Total RNA from cells was isolated using the RNeasy Mini Kit (Qiagen, Valencia, CA). First-strand cDNA was synthesized using the ReverTra Ace qPCR RT kit (#FSQ-101, Toyobo, Osaka, Japan). RT–qPCR was performed

by using Brilliant SYBR Green QPCR Master Mix (Agilent Technologies, Palo Alto, CA), and the following PCR conditions were used: 95 °C for 3 min, followed by 40 cycles of 95 °C for 5 s and 60 °C for 30 s, and followed by 95 °C for 15 s and 60 °C for 60 s melt curve analysis to check amplification specificity, using Quantstudio3 instrument (Applied Biosystems, Foster City, CA). The absolute level of each GPCR cDNA was measured by using a standard curve generated with the GPCR plasmid template and gene-specific primers. The primer sequences used are: CXCR4: 5'-CCACCATCTACTCCATCATCTTC-3' and 5'-ACTTGTCCTGTCATGCTTCTC-3'; HRH1: 5'-CCTCTGCTGGATCCCTTATTTTC-3' and 5'-GGTTCAGTGTGGAGTTGATGTA-3'; HRH2: 5'-AGTGCA AAGTCCAGGTCAAT-3' and 5'-GAAGATGCGGTAGTAGGTGATG-3'; HRH3: 5'-CTGCTATGCCGAGTT CTTCTAC-3' and 5'-GATGTTTCAGGTAGATGCTGAGG-3'; HRH4: 5'-TCCTTGCCATCACATCATTCT-3' and 5'-CTACTGAGATGATCACGCTTCC-3'; and GAPDH: 5'-ATGACATCAAGAAGGTGGTGAA-3' and 5'-GCT GTTGAAGTCAGAGGAGAC-3'.

Transwell migration assay

Cell migration was assayed in 24-well cell culture plates using transwell inserts with 8 µm pore membranes (#3422, Corning). Transwell inserts were precoated with collagen I (50 µg/mL). MDA-MB-231 cells were seeded at 80% confluency in 60 mm cell culture dishes. The next day, the cells were serum-starved overnight. Then, the cells were detached and resuspended (1 or 2 × 10⁵ cells/mL) in assay buffer (0.5% BSA in RPMI 1640). After incubation for 3 h, cells on the lower surface of the transwell inserts were fixed with 4% paraformaldehyde and stained with crystal violet. Stained cells were counted in at least 10 different fields under light microscopy (×200 magnification).

Flow cytometry

Cells were detached using PBS containing 10 mM EDTA and labeled with mouse anti-CXCR4 primary antibody (#4G10, Santa Cruz Biotechnology, Santa Cruz, CA), mouse anti-HRH1 monoclonal antibody provided by Dr. Hosun Son (GPCR Therapeutics, Seoul, Korea), or rabbit anti-HA monoclonal antibody (#3724, Cell Signaling Technology). An APC-conjugated goat anti-mouse IgG antibody (R&D Systems, Abingdon, UK) was used to label CXCR4 and HRH1, and goat anti-rabbit IgG-Alexa Fluor 488 antibody (#A32731, Invitrogen) was used to label HA tag. Cells were analyzed with a FACS Canto II (BD Biosciences, San Jose, CA).

Expression and survival analysis

To evaluate the association between CXCR4 and HRH1 expression and prognosis in breast cancer, publicly available datasets from TCGA database were analyzed. The expression and clinical data of TCGA Breast Invasive Carcinoma (BRCA) were downloaded from the UCSC Xena Browser (<https://xenabrowser.net/>). Both violin plots for expression data and Kaplan–Meier survival curves were analyzed using R version 4.1.2 (<http://www.r-project.org/>).

Statistical analysis

Statistical significance was determined by one-way ANOVA followed by Tukey's multiple comparison test, and two-way ANOVA followed by Bonferroni's multiple comparison test using GraphPad Prism software (GraphPad Software, San Diego, CA).

Data availability

Cancer cell line RNA-seq data were downloaded from the CCLE (<https://sites.broadinstitute.org/ccle/>). The expression and clinical data of TCGA were downloaded from the UCSC Xena Browser (<https://xenabrowser.net/>). All data generated or analyzed during this study are included in this published article and its Supplementary Information files.

Received: 31 October 2022; Accepted: 19 January 2023

Published online: 02 February 2023

References

- Pierce, K. L., Premont, R. T. & Lefkowitz, R. J. Seven-transmembrane receptors. *Nat. Rev. Mol. Cell Biol.* **3**, 639–650 (2002).
- Hausser, A. S. *et al.* Pharmacogenomics of GPCR drug targets. *Cell* **172**, 41–54 e19 (2018).
- Rask-Andersen, M., Masuram, S. & Schioth, H. B. The druggable genome: Evaluation of drug targets in clinical trials suggests major shifts in molecular class and indication. *Annu. Rev. Pharmacol. Toxicol.* **54**, 9–26 (2014).
- Santos, R. *et al.* A comprehensive map of molecular drug targets. *Nat. Rev. Drug Discov.* **16**, 19–34 (2017).
- Dorsam, R. T. & Gutkind, J. S. G-protein-coupled receptors and cancer. *Nat. Rev. Cancer* **7**, 79–94 (2007).
- Klein, R. S. & Rubin, J. B. Immune and nervous system CXCL12 and CXCR4: Parallel roles in patterning and plasticity. *Trends Immunol.* **25**, 306–314 (2004).
- Griffith, J. W., Sokol, C. L. & Luster, A. D. Chemokines and chemokine receptors: positioning cells for host defense and immunity. *Annu. Rev. Immunol.* **32**, 659–702 (2014).
- Müller, A. *et al.* Involvement of chemokine receptors in breast cancer metastasis. *Nature* **410**, 50–56 (2001).
- Hall, J. M. & Korach, K. S. J. M. E. Stromal cell-derived factor 1, a novel target of estrogen receptor action, mediates the mitogenic effects of estradiol in ovarian and breast cancer cells. *Mol. Endocrinol.* **17**, 792–803 (2003).
- Taichman, R. S. *et al.* Use of the stromal cell-derived factor-1/CXCR4 pathway in prostate cancer metastasis to bone. *Cancer Res.* **62**, 1832–1837 (2002).
- Kim, S. Y. *et al.* Inhibition of the CXCR4/CXCL12 chemokine pathway reduces the development of murine pulmonary metastases. *Clin. Exp. Metastasis* **25**, 201–211 (2008).
- Geminder, H. *et al.* A possible role for CXCR4 and its ligand, the CXC chemokine stromal cell-derived factor-1, in the development of bone marrow metastases in neuroblastoma. *J. Immunol.* **167**, 4747–4757 (2001).

13. Porvasnik, S. *et al.* Effects of CXCR4 antagonist CTCE-9908 on prostate tumor growth. *Prostate* **69**, 1460–1469 (2009).
14. Orimo, A. *et al.* Stromal fibroblasts present in invasive human breast carcinomas promote tumor growth and angiogenesis through elevated SDF-1/CXCL12 secretion. *Cell* **121**, 335–348 (2005).
15. Ying, J., Xu, Q., Zhang, G., Liu, B. & Zhu, L. The expression of CXCL12 and CXCR4 in gastric cancer and their correlation to lymph node metastasis. *Med. Oncol.* **29**, 1716–1722 (2012).
16. Mukherjee, D. & Zhao, J. The Role of chemokine receptor CXCR4 in breast cancer metastasis. *Am. J. Cancer Res.* **3**, 46–57 (2013).
17. Chatterjee, S., Behnam Azad, B. & Nimmagadda, S. The intricate role of CXCR4 in cancer. *Adv. Cancer Res.* **124**, 31–82 (2014).
18. Otsuka, S. *et al.* CXCR4 overexpression is associated with poor outcome in females diagnosed with stage IV non-small cell lung cancer. *J. Thorac. Oncol.* **6**, 1169–1178 (2011).
19. Xu, C. *et al.* CXCR4 overexpression is correlated with poor prognosis in colorectal cancer. *Life Sci.* **208**, 333–340 (2018).
20. Domanska, U. M. *et al.* A review on CXCR4/CXCL12 axis in oncology: No place to hide. *Eur. J. Cancer* **49**, 219–230 (2013).
21. Jung, Y. *et al.* Recruitment of mesenchymal stem cells into prostate tumours promotes metastasis. *Nat. Commun.* **4**, 1795 (2013).
22. Scarlett, K. A. *et al.* Agonist-induced CXCR4 and CB2 Heterodimerization Inhibits Gα13/RhoA-mediated Migration. *Mol. Cancer Res.* **16**, 728–739 (2018).
23. Coke, C. J. *et al.* Simultaneous activation of induced heterodimerization between CXCR4 chemokine receptor and cannabinoid receptor 2 (CB2) reveals a mechanism for regulation of tumor progression. *J. Biol. Chem.* **291**, 9991–10005 (2016).
24. Decaillet, F. M. *et al.* CXCR7/CXCR4 heterodimer constitutively recruits beta-arrestin to enhance cell migration. *J. Biol. Chem.* **286**, 32188–32197 (2011).
25. Thangam, E. B. *et al.* The role of histamine and histamine receptors in mast cell-mediated allergy and inflammation: The hunt for new therapeutic targets. *Front. Immunol.* **9**, 1873 (2018).
26. Garcia-Caballero, M., Neugebauer, E., Campos, R., Nunez de Castro, I. & Vara-Thorbeck, C. Increased histidine decarboxylase (HDC) activity in human colorectal cancer: Results of a study on ten patients. *Agents Actions* **23**, 357–360 (1988).
27. Garcia-Caballero, M., Neugebauer, E., Rodriguez, F., Nunez de Castro, I. & Vara-Thorbeck, C. Histamine synthesis and content in benign and malignant breast tumours. Its effects on other host tissues. *Surg. Oncol.* **3**, 167–173 (1994).
28. Chanda, R. & Ganguly, A. K. Diamine-oxidase activity and tissue di- and poly-amine contents of human ovarian, cervical and endometrial carcinoma. *Cancer Lett.* **89**, 23–28 (1995).
29. Hegyesi, H. *et al.* Suppression of melanoma cell proliferation by histidine decarboxylase specific antisense oligonucleotides. *J. Invest. Dermatol.* **117**, 151–153 (2001).
30. Graff, L. *et al.* Expression of histidine decarboxylase and synthesis of histamine by human small cell lung carcinoma. *Am. J. Pathol.* **160**, 1561–1565 (2002).
31. Cianchi, F., Vinci, M. C. & Masini, E. Histamine in cancer: The dual faces of the coin. *Cancer Biol. Ther.* **7**, 36–37 (2008).
32. Valencia, S., Hernandez-Angeles, A., Soria-Jasso, L. E. & Arias-Montano, J. A. Histamine H(1) receptor activation inhibits the proliferation of human prostatic adenocarcinoma DU-145 cells. *Prostate* **48**, 179–187 (2001).
33. Zhao, J. *et al.* Upregulation of histamine receptor H1 promotes tumor progression and contributes to poor prognosis in hepatocellular carcinoma. *Oncogene* **39**, 1724–1738 (2020).
34. Ghandi, M. *et al.* Next-generation characterization of the cancer cell line encyclopedia. *Nature* **569**, 503–508 (2019).
35. Hu, C. D., Chinenov, Y. & Kerppola, T. K. Visualization of interactions among bZIP and Rel family proteins in living cells using bimolecular fluorescence complementation. *Mol. Cell* **9**, 789–798 (2002).
36. Vila-Coro, A. J. *et al.* The chemokine SDF-1alpha triggers CXCR4 receptor dimerization and activates the JAK/STAT pathway. *FASEB J.* **13**, 1699–1710 (1999).
37. Babcock, G. J., Farzan, M. & Sodroski, J. Ligand-independent dimerization of CXCR4, a principal HIV-1 coreceptor. *J. Biol. Chem.* **278**, 3378–3385 (2003).
38. Mercier, J. F., Salahpour, A., Angers, S., Breit, A. & Bouvier, M. Quantitative assessment of beta 1- and beta 2-adrenergic receptor homo- and heterodimerization by bioluminescence resonance energy transfer. *J. Biol. Chem.* **277**, 44925–44931 (2002).
39. Couturier, C. & Jockers, R. Activation of the leptin receptor by a ligand-induced conformational change of constitutive receptor dimers. *J. Biol. Chem.* **278**, 26604–26611 (2003).
40. Agle, K. A., Vongsa, R. A. & Dwinell, M. B. Calcium mobilization triggered by the chemokine CXCL12 regulates migration in wounded intestinal epithelial monolayers. *J. Biol. Chem.* **285**, 16066–16075 (2010).
41. Mellado, M., Rodriguez-Frade, J. M., Manes, S. & Martinez, A. C. Chemokine signaling and functional responses: The role of receptor dimerization and TK pathway activation. *Annu. Rev. Immunol.* **19**, 397–421 (2001).
42. Bendall, L. J., Baraz, R., Juarez, J., Shen, W. & Bradstock, K. F. Defective p38 mitogen-activated protein kinase signaling impairs chemotactic but not proliferative responses to stromal-derived factor-1alpha in acute lymphoblastic leukemia. *Cancer Res.* **65**, 3290–3298 (2005).
43. Hill, S. J. Distribution, properties, and functional characteristics of three classes of histamine receptor. *Pharmacol. Rev.* **42**, 45–83 (1990).
44. Leurs, R., Smit, M. J. & Timmerman, H. Molecular pharmacological aspects of histamine receptors. *Pharmacol. Ther.* **66**, 413–463 (1995).
45. Roland, J. *et al.* Role of the intracellular domains of CXCR4 in SDF-1-mediated signaling. *Blood* **101**, 399–406 (2003).
46. Klein, R. S. *et al.* SDF-1 alpha induces chemotaxis and enhances Sonic hedgehog-induced proliferation of cerebellar granule cells. *Development* **128**, 1971–1981 (2001).
47. Pfeil, E. M. *et al.* Heterotrimeric G protein subunit Galphaq is a master switch for Gbetagamma-mediated calcium mobilization by Gi-Coupled GPCRs. *Mol. Cell* **80**, 940–954 e946 (2020).
48. Olumi, A. F. *et al.* Carcinoma-associated fibroblasts direct tumor progression of initiated human prostatic epithelium. *Cancer Res.* **59**, 5002–5011 (1999).
49. Gao, Z., Wang, X., Wu, K., Zhao, Y. & Hu, G. Pancreatic stellate cells increase the invasion of human pancreatic cancer cells through the stromal cell-derived factor-1/CXCR4 axis. *Pancreatol.* **10**, 186–193 (2010).
50. Cojoc, M. *et al.* Emerging targets in cancer management: Role of the CXCL12/CXCR4 axis. *Oncol. Targets Ther.* **6**, 1347–1361 (2013).
51. Sotsios, Y., Whittaker, G. C., Westwick, J. & Ward, S. G. The CXC chemokine stromal cell-derived factor activates a Gi-coupled phosphoinositide 3-kinase in T lymphocytes. *J. Immunol.* **163**, 5954–5963 (1999).
52. Nanki, T. & Lipsky, P. E. Stimulation of T-Cell activation by CXCL12/stromal cell derived factor-1 involves a G-protein mediated signaling pathway. *Cell. Immunol.* **214**, 145–154 (2001).
53. Cricco, G. *et al.* Histamine regulates the MAPK pathway via the H(2) receptor in PANC-1 human cells. *Inflamm. Res.* **53**(Suppl 1), S65–66 (2004).
54. Rivera, E. S. *et al.* Histamine as an autocrine growth factor: An unusual role for a widespread mediator. *Semin. Cancer Biol.* **10**, 15–23 (2000).
55. Lázár-Molnár, E. *et al.* Inhibition of human primary melanoma cell proliferation by histamine is enhanced by interleukin-6. *Eur. J. Clin. Invest.* **32**, 743–749 (2002).
56. Medina, V. *et al.* The role of histamine in human mammary carcinogenesis: H3 and H4 receptors as potential therapeutic targets for breast cancer treatment. *Cancer Biol. Ther.* **7**, 28–35 (2008).

57. Rudolph, M. I. *et al.* The influence of mast cell mediators on migration of SW756 cervical carcinoma cells. *J. Pharmacol. Sci.* **106**, 208–218 (2008).
58. Shi, Z. *et al.* Distinct roles of histamine H1- and H2-receptor signaling pathways in inflammation-associated colonic tumorigenesis. *Am. J. Physiol. Gastrointest. Liver Physiol.* **316**, G205–G216 (2019).
59. Parsons, M. E. & Ganellin, C. R. Histamine and its receptors. *Br. J. Pharmacol.* **147**(Suppl 1), S127–135 (2006).
60. Saka, Y., Hagemann, A. I., Piepenburg, O. & Smith, J. C. Nuclear accumulation of Smad complexes occurs only after the midblastula transition in *Xenopus*. *Development* **134**, 4209–4218 (2007).

Acknowledgements

We thank Dr. Hosun Son (GPCR Therapeutics, Seoul, Korea) for generously providing mouse anti-HRH1 monoclonal antibody. We are also grateful to Dr. Pina M. Cardarelli and the members of the Huh lab for helpful comments and discussions. This work was supported by GPCR Therapeutics Inc. and the National Research Foundation of Korea (2020R1A5A1018081).

Author contributions

C.P., D.S.S., J.Y.J., and W.K.H. conceived and designed experiments. C.P., J.W.L., and K.K. performed experiments. C.P., J.W.L., K.K., D.S.S., J.Y.J., and W.K.H. analyzed data. C.P., J.Y.J., and W.K.H. wrote the manuscript. All authors reviewed and commented on the manuscript and approved the final version.

Competing interests

C.P., D.S.S., and J.Y.J. are employees of GPCR Therapeutics Inc. D.S.S. and W.K.H. are shareholders in GPCR Therapeutics Inc. J.W.L. and K.K. declare no competing interests.

Additional information

Supplementary Information The online version contains supplementary material available at <https://doi.org/10.1038/s41598-023-28531-1>.

Correspondence and requests for materials should be addressed to J.-Y.J. or W.-K.H.

Reprints and permissions information is available at www.nature.com/reprints.

Publisher's note Springer Nature remains neutral with regard to jurisdictional claims in published maps and institutional affiliations.



Open Access This article is licensed under a Creative Commons Attribution 4.0 International License, which permits use, sharing, adaptation, distribution and reproduction in any medium or format, as long as you give appropriate credit to the original author(s) and the source, provide a link to the Creative Commons licence, and indicate if changes were made. The images or other third party material in this article are included in the article's Creative Commons licence, unless indicated otherwise in a credit line to the material. If material is not included in the article's Creative Commons licence and your intended use is not permitted by statutory regulation or exceeds the permitted use, you will need to obtain permission directly from the copyright holder. To view a copy of this licence, visit <http://creativecommons.org/licenses/by/4.0/>.

© The Author(s) 2023, corrected publication 2024